



# University of HUDDERSFIELD

## University of Huddersfield Repository

Rajput, N.S., Tong, Zhen, Verma, H.C. and Luo, X.

Ion-beam-assisted fabrication and manipulation of metallic nanowires

### Original Citation

Rajput, N.S., Tong, Zhen, Verma, H.C. and Luo, X. (2015) Ion-beam-assisted fabrication and manipulation of metallic nanowires. *Micro & Nano Letters*, 10 (7). pp. 334-338. ISSN 1750-0443

This version is available at <http://eprints.hud.ac.uk/25255/>

The University Repository is a digital collection of the research output of the University, available on Open Access. Copyright and Moral Rights for the items on this site are retained by the individual author and/or other copyright owners. Users may access full items free of charge; copies of full text items generally can be reproduced, displayed or performed and given to third parties in any format or medium for personal research or study, educational or not-for-profit purposes without prior permission or charge, provided:

- The authors, title and full bibliographic details is credited in any copy;
- A hyperlink and/or URL is included for the original metadata page; and
- The content is not changed in any way.

For more information, including our policy and submission procedure, please contact the Repository Team at: [E.mailbox@hud.ac.uk](mailto:E.mailbox@hud.ac.uk).

<http://eprints.hud.ac.uk/>

# Ion beam assisted fabrication and manipulation of metallic nanowires

N. S. Rajput<sup>1,2</sup>, Z. Tong<sup>2</sup>, H. C. Verma<sup>1</sup> and X. Luo<sup>2</sup>

<sup>1</sup> Department of Physics, Indian Institute of Technology Kanpur, Kanpur 208016, India

<sup>2</sup> Department of Design, Manufacture and Engineering Management, University of Strathclyde, Glasgow G1 1XQ, United Kingdom  
E-mail: xichun.luo@strath.ac.uk

Metallic nanowires are the key performers for future micro/nano devices. Controlled maneuver and integration of such nanoscale entities are in high demand. In this letter, we discuss about a fabrication approach that combines chemical etching and ion beam milling to fabricate metallic nanowires. The shape modification of the metallic nanowires using ion beam irradiation (bending towards the ion beam side) is investigated. The bending effect of the nanowires is observed to be instantaneous and permanent. The ion beam assisted shape maneuver of the metallic structures is studied in the light of ion induced vacancy formation and reconfiguration of the damaged layers. The manipulation method can be used in fabricating structures of desired shape and aligning structures at a large scale. The controlled bending method of the metallic nanowires also provides an understanding of the strain formation process in nanoscale metals.

**1. Introduction:** Nanowires (NWs) have 1D structure with various excellent size dependent properties and have immense applications e.g., in sensor technology, nanoelectronics, energy, photonics, environment, etc. They (NWs) are recognized as the building blocks of the next generation micro/nano electronic devices [1-4]. Various fabrication techniques have been developed by several research groups to fabricate NWs [3-10]. However, as compared to the research on developing varieties of NWs, the extent of application-oriented research on NWs is limited. The reason could be the challenges encountered in handling and integration of the nanoscale features with relatively larger units or devices.

In recent decades, various integration approaches have been proposed. Wu et al. demonstrated an approach to grow organic NWs on Au coated areas through a surface energy induced process [11]. Patterned growth of the NW arrays and in-situ device integration were achieved by manipulating the Au electrode geometries. Peng et al. developed a welding process for assembling nanoscale objects, where the nanomanipulator probes were used to deposit nanoscale volume of a predefined material by Joule heating method [12]. Moreover, direct manipulation of NWs using nanomanipulator and atomic force microscopy tip has also been carried out [13, 14]. The site-specific programmable growth technique to grow branched Si NWs, discussed by Jun et al. can lead to the development of a reliable nanoscale maneuver and integration technique [15]. Based on the Bosch process, Arkan et al. has proposed another technique for the fabrication and integration of Si NWs with microscale metallic electrodes/contacts [16]. These studies show a promising start in the development of manipulation and integration approaches for NWs with micron entities; however, in order to meet the challenges in designing the future micro/nano scale devices, it is necessary to develop a versatile, material independent, and precisely controllable (with nanometric resolution) manipulating and integration method for NWs.

In this article, we present the work on ion induced shape modification process of metallic NWs. Though there are several popular and low cost methods are available [4, 9, 10], we have implemented a different approach in order to create the NWs. A combined process of chemical etching and ion beam milling has been used in order to fabricate the metallic nanowires. This fabrication approach has a unique advantage. The fabrication procedure during the ion beam milling can be monitored in-situ and thus the wire thickness can be controlled easily. The ion matter interactions during the controlled shape modification of the metallic nanostructures are studied. The ion beam assisted shape modification (Ion induced manipulation (IIM)) method has potential application in fabricating structures of desired shape as well as in assembling and editing micro/nano electronics.

The fabricated and manipulated NWs can be used in Scanning Probe Microscopy (SPM) as a probe tip, where the resolution is often defined by the tip geometry. The high aspect ratio of the probe (i.e. the NW) can provide extra benefit in terms of examining deep vertical structure without considerable artifacts. The metallic NWs can also be used as field emitting tips. The additional IIM process can provide the desired geometry easily.

**2. Materials and methods:** High quality, corrosion resistant metallic wires (Heraeus make) were used for the experiment. The diameters of the wires were 17 – 40  $\mu\text{m}$ . In order to thin down the wires from micron to nano dimension, a two-stage step-by-step processing approach was used. Initially, the wires were thinned down to few microns ( $\sim 5 \mu\text{m}$ ) using specific chemical etching processes and further reduction to few tens of nm was achieved using ion beam milling process. These processes are discussed below.

## A. Step I: Chemical etching

The metallic wires (diameter: 17 – 40  $\mu\text{m}$ ) were taken and immersed in acid solutions in order to thin down the diameter. The etching solutions were prepared using commercially available chemical reagents (Rankem, RFCL Ltd.). For etching Al wires (discussed in this article), solution was prepared with the available HCl reagent, diluted with  $\sim 60\%$   $\text{H}_2\text{O}$ . The wires were kept in the etching solution to thin the wire diameter down to few  $\mu\text{m}$  (Fig. 1). The thinned wires, feebly visualized by naked eye, can be properly inspected in Scanning Electron Microscope (SEM). The thinned wires were held by fine tweezer and rinsed with deionized water to clean and remove any unwanted substance from the wires' surfaces.

The part of a wire that was thinned down by the etching process was gently gripped with the help of a fine tweezer and one end of the wire was glued to an Al stub with the other end hanging freely. Conductive Silver paint (Leitsilber 200, Ted Pella Inc.) was used to glue the wire with the stub and kept in ambient air for  $\sim 5$  min to dry out properly. The use of silver solution also ensures a proper electrical grounding of the wire (Fig. 1). Subsequently, the prepared sample (the wire along with the stub) was taken and placed inside a Focused Ion Beam (FIB) chamber for further thinning down of the wire.

## B. Step II: Ion beam milling

Dual beam FIB systems (Nova 600 NanoLab and Nova 200 NanoLab, FEI make) were used for the experiments. The systems employ Ga Liquid Metal Ion Sources (LMISs) to produce high quality beam of singly charged Ga ions and Sirion type Field Emission Guns (FEGs) to generate high-resolution electron beams.

The free end of the wire was irradiated from the top direction with high beam current of  $\sim 20$  nA (applied beam voltage: 30 kV) as shown in the Fig. 1c. Because of the sputtering process (material removal due to ion beam irradiation), the thickness of the wire got further reduced. As the wire got reduced to  $\sim 1$   $\mu\text{m}$ , the beam current was also reduced and set at 10 – 50 pA for fine milling. As the diameter of the wire got reduced further, the nanowire started moving towards the ion beam direction due to ion induced bending process (discussed in details in the following section) and produced a sharp angle with the rest of the unirradiated wire (Fig. 1d). Sputtering and bending using controlled irradiation resulted in the formation of a fine nanowire being fabricated at the edge of a relatively thicker wire.

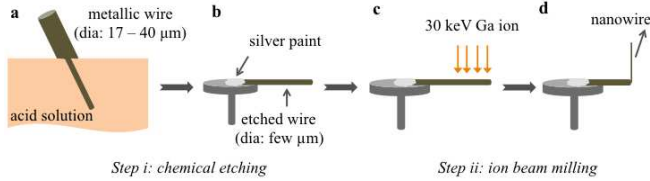


Fig. 1 The schematic picture shows the steps to fabricate a metallic nanowire.

- A Metallic wire (diameter: 17 – 40  $\mu\text{m}$ ) is partially immersed in an acid solution for etching.
- One end of the etched part of the wire (diameter  $\sim$  few  $\mu\text{m}$ ) is glued with a metallic stub with the other end hanging freely.
- The sample (metallic stub with the glued wire) is taken inside the FIB chamber and further irradiated by 30 keV Ga ions to thin down the wire.
- The fabricated nanowire. The structure makes a sharp angle with the rest due to the ion induced bending process.

**3. Results and discussion:** SEM image of an Al nanowire fabricated using the above approach is shown in Fig. 2. Inset image shows the zoomed-in part of the fabricated nanowire. The image was taken at 15 keV beam energy,  $2.2 \times 10^8$  electrons  $\mu\text{m}^{-2} \text{s}^{-1}$  beam flux, and 100 ns beam dwell time. During the SEM scanning, charges can get accumulated in the wire and may affect the SEM image formation process. As a result, the perception of the wire thickness and shape in the SEM image may differ from the actual size and shape. This is discussed in details in the following section.

#### A. Imaging and charging effect

Another example of a nanowire fabricated using the above-mentioned processes is shown in Fig. 3a. The diameter of the wire is  $\sim 25$  nm. The nanowire has several curves in different portions of the structure. SEM images of the nanowire (Fig. 3) were taken at the applied beam voltage of 15 kV and beam flux of  $1.9 \times 10^8$  electrons  $\mu\text{m}^{-2} \text{s}^{-1}$ . Fig. 3a was taken at a relatively low beam dwell time ( $t_d$ ) of 100 ns. A bright region (dotted portion in the image) appears in the image. The same nanowire imaged at beam dwell time of 1  $\mu\text{s}$  is shown in Fig. 3b. The bright layer seems to diminish in this case and nearly disappears when the beam dwell time was increased to 10  $\mu\text{s}$  (Fig. 3c).

During the beam scanning, large amount of charges will accumulate on the NW as it requires finite amount of time ( $t_f$ ) to get discharged through the base region of the nanowire and the sample stub.  $t_f$  depends on the amount of charge and the channel through which it gets discharged i.e., the wire. Thus, the wire diameter can immensely affect in the discharging process of the accumulated charges.

At fast scanning mode (low  $t_d$ ), when  $t_d < t_f$ , the accumulated charge could not get sufficient time to discharge and as a result, the charging effect (the bright layer) appears in the wire (as shown in the Fig. 3a). However, when the scanning speed is slowed down sufficiently, the accumulated charges find sufficient time to get

discharged and as a result, the bright region nearly disappears (Fig. 3c). The nanowire finally seems to have a uniform thickness throughout its length.

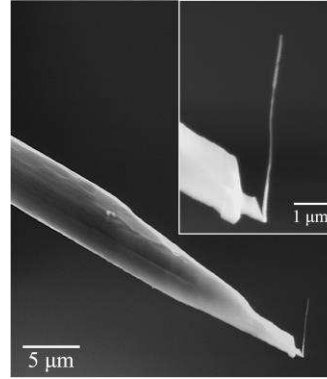


Fig. 2 SEM image of a nanowire fabricated using a combined process of chemical etching and ion beam milling. Inset shows a zoomed-in view of the fabricated structure.

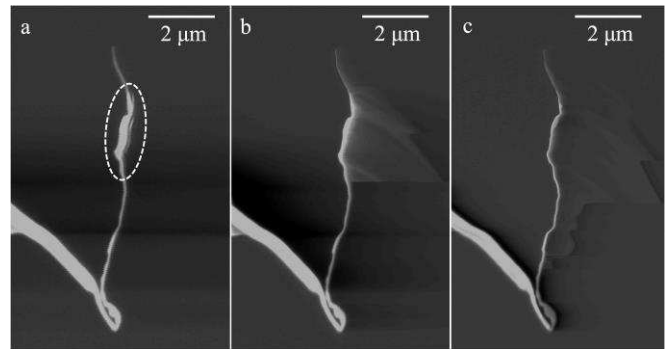


Fig. 3 SEM images of a nanowire taken at the applied beam voltage of 15 kV.

- Was taken at the beam dwell time ( $t_d$ ) of 100 ns. The portion encircled with dotted line shows the charging effect.
- Was taken at  $t_d = 1$   $\mu\text{s}$ , and
- Was taken at  $t_d = 10$   $\mu\text{s}$ .

#### B. Ion induced manipulation (IIM) and its mechanism

The fabricated metallic nanowire (Al) was subjected to 30 keV Ga ion beam as illustrated in Fig. 4a. The irradiation was made at an incident angle of  $\sim 45^\circ$  with the irradiated flux of  $5.6 \times 10^6$  ions  $\mu\text{m}^{-2} \text{s}^{-1}$ . The arrow lines in the figure show the direction of the ion beam irradiation. Fig. 4b-d shows the SEM snapshots, taken after every 2 – 3 frames of ion beam scanning. The snapshots show the gradual bending of the nanowire towards the ion beam direction. The deviation of the nanowire from its initial position is termed as  $\theta$  and the measured values are shown in the figures. The bending process is found to be instantaneous and permanent. The “permanent” behavior of the bending process infers the plastic nature of the process. The evolution of the bending process is shown in Fig. 4e by overlapping all the images 4a-d. Fig. 4e shows an important feature of the bending of the NW. The base part of the fabricated NW is found to bend considerably as compared to the other portion of the NW.

Ion induced bending process has been observed by various groups in different nanoscale materials. The bending of carbon nanotube [17], nanowires [18-21], carbon nanopillar [22], biological structure [23], thin film structures [24], metallic cantilever [25] are reported and various mechanisms have been proposed to explain this nanoscale phenomenon. Some of the observed bending processes are discussed on the basis of ion induced damage formation [17-19, 21, 24],

whereas in few materials the process has been discussed on the basis of thermal stress developed during ion beam irradiation [22, 23].

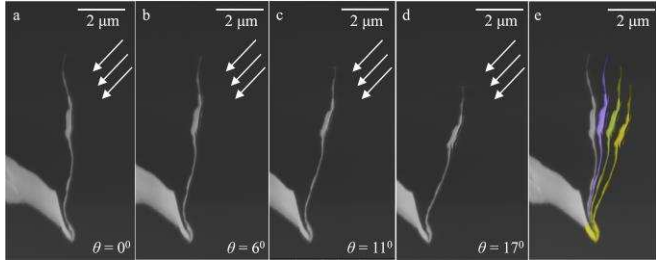


Fig. 4 SEM images showing the bending process. a-d SEM images show the bending process of the metallic nanowire (Al NW) as a result of ion beam irradiation. The arrows indicate the direction of the ion beam irradiation. The bending angle ( $\theta$ ) enunciates the deflection of the NW with respect to its initial position. e Overlapped images show the evolution of the irradiated NW.

In order to understand the bending phenomenon observed in metallic NWs, an atomistic investigation with the help of a Monte Carlo (MC) program is carried out. When an ion particle enters into the solid material, it interacts with the target atoms and transfers its energy and momentum to the nuclei and electrons of the target atoms. As a result of the collision process, large amount of voids are produced within the interaction region. The interaction process also causes some surface atoms to come out from the material. The amount of voids (vacancies) and sputtering yield highly depends on the incident beam energy, incident angle, the beam type and the target material [26]. In addition to the surface damage and sputtering of the surface atoms, the Ga ions are likely to be doped in the NW. The volumetric change in the NW due to this implantation may be thought to initiate the bending process. In order to bend the NW towards the ion beam side, heavy amount of Ga ions should be implanted on the opposite side of the NWs. The range of the implanted Ga ions irradiated at  $45^\circ$  in the Al NW, calculated by SRIM [27] (a MC based program) is about 15 nm (whereas the diameter of the NW is  $\sim 25$  nm). So a heavy concentration of implanted Ga ions on the rear surface is unlikely. Moreover, as the NW gradually bends, the irradiated angle changes ( $\theta$  increases) and the implanted range decreases [27]. Despite the changes in the implantation ranges of the Ga ions in the NW with  $\theta$ , the wire bends towards the beam direction. Irradiating with low energetic Ga ions on a NW (where the implantation depth is much lower than the wire diameter) also shows bending of the NW towards the ion beam side. The experiments carried out on relatively thicker NWs also show the typical bending of the NWs towards the ion beam side. These observations suggest that the volumetric change caused by the implantation has no significant role in the bending process of these structures.

SRIM results show that irradiating 30 keV Ga ions at an incident angle of  $45^\circ$  on the Al substrate can create vacancies of  $\sim 326$  per ion and surface sputtering of  $\sim 9$  atoms ion $^{-1}$ . Kinchin-Pease model is used to calculate the damages. The vacancies are created mostly at the surface level, within  $\sim 15$  nm from the sample surface as shown in Fig. 5. Thus, large number of vacancies and defects are created at the surface layers facing the ion beam. The disturbed/perturbed atoms at the surface layers tend to settle down in a much stable configuration through a reconfiguration process.

Ion beam can also produce significant amount of temperature, which can accelerate the reconfiguration process. MC calculation shows that during the interaction of 30 keV Ga ions with the Al substrate irradiated at  $45^\circ$  incident angle,  $\sim 65\%$  of the ion beam energy is converted into phonon generation, mostly contributed by the recoils [27]. Thus, a single ion can raise the temperature to  $\sim 350^\circ\text{C}$

within the interaction region. A fraction of heat will be added from the ionization of the electrons as well. As a result, the final temperature is expected to be more than this value. With the subsequent ion beam irradiation, the total temperature is likely to increase. However, there is also dissipation of heat through conduction and radiation. As a result of the dynamic process of heat generation by the ion irradiation and dissipation through conduction and radiation, an equilibrium temperature would be maintained. In order to calculate the saturated heat precisely, a proper nanoscale heat transport mechanism has to be developed. However, as the preliminary calculation enunciates (raise of temperature to  $\sim 350^\circ\text{C}$  within the interaction region by a single ion), the temperature raised by the ion beam within the collision cascade region is sufficient to initiate the recrystallization process in the nanowire [28].

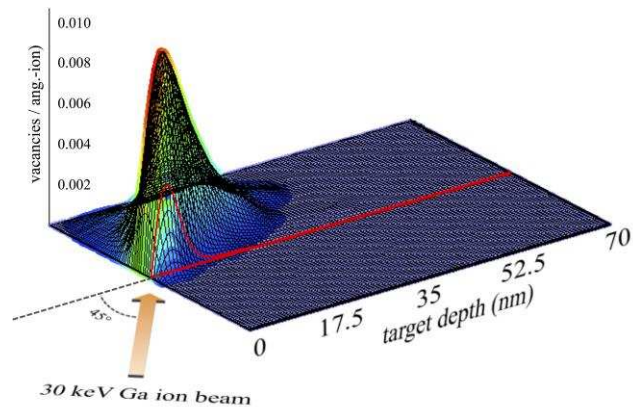


Fig. 5 Shows the 3D vacancy profile in Al material created by 30 keV Ga ions irradiated at  $45^\circ$ .

As a result of the reconfiguration process, different amounts of stresses are developed across the layers of the system. Schematic Fig. 6 shows the formation of stresses in the NW as a result of the ion beam irradiation. When the surface layers facing the ion beam (L1) shrink in order to release the stress, this will subsequently affect the connected neighboring layers (the layers, L2, which are not receiving ion beam irradiation but connected with the L1 layers though the atomic bonds) and a new equilibrium shape is achieved with the structure bending towards the ion beam direction. Fig. 6 shows the schematic representation of the bending process; describing the process of ion beam irradiation, subsequent development of compressive and tensile stresses across the surface layers and bending of the nanowire.

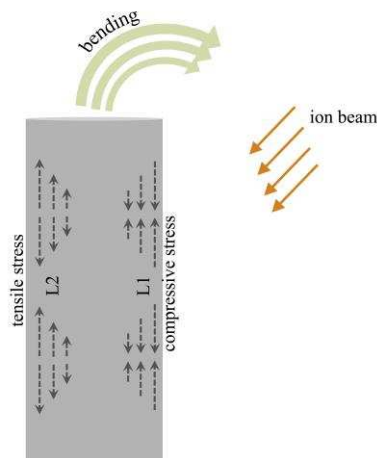


Fig. 6 A schematic picture showing the development of compressive and tensile stress as a result of ion beam irradiation and subsequent bending of the nanowire.

The amount of damage formation and reconfiguration process in a NW depends on the amount of irradiation received, irradiation angle as well as on the size of the structure; thus, the bending tendency (an outcome of damage formation and recrystallization) of an irradiated structure also depends of these parameters. Due to several curves in the NW (Fig. 4), the NW receives ununiform irradiation throughout its surface. The base portion might have received relatively larger irradiation (due to its geometry) to cause higher tendency of bending and as a result, bending at the base region is comparatively higher than other portions. Due to uneven reception of irradiation by the NW throughout its length, the amount of curvatures also gradually decreases.

The dynamic process of the ion beam induced damage formation and heat generation, dissipation of the heat, subsequent reconfiguration of the damaged layers and stress development across the layers requires a broader theoretical modeling in order to quantify the bending process precisely. Further theoretical investigation on the IIM process will be taken in a future project.

### C. IIM in other systems

Few Cu NWs were fabricated using the same fabrication approach discussed in this article. Subsequently, the fabricated NWs were exposed to the high energetic Ga ions at a particular incidence angle. Similar pattern of bending has also been observed in this case. The shape modification of a Cu NW during the 30 keV Ga ion beam irradiation is shown in Fig. 7a-c. The irradiation was made from the top direction.

The top-down fabrication approach employed in FIB processing (ion beam milling) can be efficiently used to fabricate nanostructures of different shape. Using this approach, few Al NWs were fabricated out of an Al substrate. SEM image of an Al NW fabricated using this approach is shown in Fig. 7d. The bending of the Al NW towards the side of the ion beam during the 16 keV ion beam irradiation is shown in the Fig. 7d-f.

Detail investigation on the dependence of bending affinity on the NW material is not investigated in this paper, however, from the understanding of the bending phenomenon which we explain on the basis of defect formation, reconfiguration process of the damaged layers, and stress generation in the system, it can be urged that even though same amount of dose are provided to different nanowires, the bending affinity would be different in different nanowires.

It is observed that bending is more pronounced wherever there is a change in the wire thickness (Fig. 7d-f) as compared to the straighter portions of the wire. This could be because of the fact that at these portions the local irradiation angle is suitable for creating maximum amount of defects, which could lead to the generation of higher amount of stress and hence higher bending tendency. The primary role of the ion induced temperature is expected to be only in the recrystallization process of the NW material. In the case of NW of varying thickness, the temperature distribution and diffusion along the NW would be inhomogeneous and hence the recrystallization process would be ununiform. This is also likely to play a key role in the ununiform bending tendency along the NW.

Experimental observations and our discussion enunciate that ion induced bending phenomenon ought to be a generic process for nanoscale crystalline/polycrystalline materials. This suggests that the IIM technique is also applicable to other nanoscale non-metallic crystalline materials.

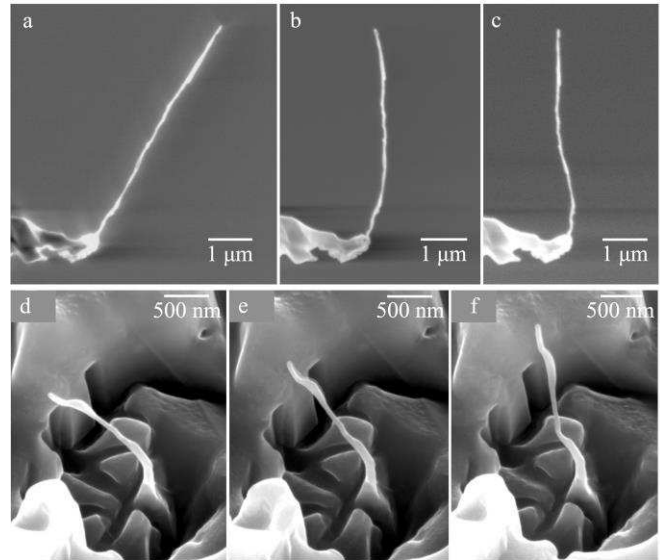


Fig. 7 SEM images of Cu and Al NWs.

a - c SEM snapshots showing the bending of a Cu NWs during the ion beam irradiation from the top direction.

d - f SEM images showing the bending of an Al NW while irradiated by the 16 keV Ga ion beam. The irradiation was made from the top direction.

**4. Conclusion:** A fabrication process that combines chemical etching and ion beam milling, to fabricate metallic nanowires is introduced in this paper. The nanowires show a tendency of bending towards the ion beam side during the ion beam irradiation. The bending phenomenon is studied on the basis of vacancy formation and reconfiguration of the damaged layers, stress formation, and releasing the stress through reshaping the structure. Our studies also show the generic nature of the IIM process in crystalline nanoscale structures and provide an understanding of strain formation process in nanoscale metals.

IIM process is instantaneous and permanent and with controlled dose, the NWs can be precisely manipulated. This opens up the feasibility of using IIM as a versatile, material independent manipulating and assembling method. The technique can find potential applications in different branches of nanotechnology. In photonics, for example, nanopillars are grown at a large scale in order to study the efficiency of metamaterials and it is seen that the efficiency depends on the angle made by the pillars with the surface. IIM, which can be used in aligning nanopillars at a large scale, can be very useful in such studies. In SEM/Transmission Electron Microscope (TEM) systems IIM can be useful in maneuvering structures selectively.

**5. Acknowledgments:** The authors acknowledge the technical support provided by the staff at Ion beam lab, IIT Kanpur and Kelvin nanocharacterization center, University of Glasgow. We are grateful to NSTI, Department of Science and Technology, India, IIT Kanpur, and EPSRC (EP/K018345/1), UK for the financial supports.

### 6. References:

- [1] Li Y., Qian F., Xiang J., Lieber C. M.: 'Nanowire electronic and optoelectronic devices', *Mater. Today*, 2006, 9, pp. 18-27.
- [2] Duan X., Huang Y., Cui Y., Wang J., Lieber C. M.: 'Indium phosphide nanowires as building blocks for nanoscale electronic and optoelectronic devices', *Nature*, 2001, 409, pp. 66-69.

- [3] Keating C. D., Natan M. J.: 'Striped Metal Nanowires as Building Blocks and Optical Tags', *Adv. Mater.*, 2003, 15, pp. 451-454.
- [4] Khalil A., Lalia B. S., Hashaikeh R., Khraisheh M.: 'Electrospun metallic nanowires: Synthesis, characterization, and applications', *J. Appl. Phys.*, 2013, 114, article id 171301, p. 16.
- [5] Dixon C. J., Curtines O. W.: 'Nanotechnology: Nanofabrication, Patterning and Self Assembly', (Nova Science Publishers, Inc., New York, 2010), pp. 237, 293, 309.
- [6] Wang Z. L.: 'Nanowires and Nanobelts: Materials, Properties and Devices-Nanowires and Nanobelts of Functional materials', (Springer, New York, 2006), pp. 21, 83, 93.
- [7] Wang H., Sun M., Ding K., Hill M. T., Ning C.: 'A Top-down Approach to Fabrication of High Quality Vertical Heterostructure Nanowire Arrays', *Nano Lett.* 2011, 11, pp. 1646-1650.
- [8] Burek M. J., Greer J. R.: 'Fabrication and Microstructure Control of Nanoscale Mechanical Testing Specimens via Electron Beam Lithography and Electroplating', *Nano Lett.*, 2010, 10, pp. 69 -76.
- [9] Liu Y., Goebel J., Yin Y.: 'Templated synthesis of nanostructured materials', *Chem. Soc. Rev.*, 2013, 42, pp. 2610-2653.
- [10] Wang Y., Angelatos A. S., Caruso F.: 'Template Synthesis of Nanostructured Materials via Layer-by-Layer Assembly', *Chem. Mater.*, 2008, 20, pp. 848-858.
- [11] Wu Y., Zhang X., Pan H., Deng W., Zhang X., Zhang X., Jie J.: 'In-situ device integration of large-area patterned organic nanowire arrays for high-performance optical sensors', *Sci. Rep.*, 2013, 3, article id 3248, p. 8.
- [12] Peng Y., Cullis T., Inkson B.: 'Bottom-up Nanoconstruction by the Welding of Individual Metallic Nanoobjects Using Nanoscale Solder', *Nano Lett.*, 2009, 9, pp. 91-96.
- [13] Conache G., Gray S., Bordag M., Ribayrol A., Fröberg L. E., Samuelson L., Pettersson H., Montelius L.: 'AFM-based manipulation of InAs nanowires', *J. Phys. Conf. Ser.*, 2008, 100, article id 052051 p. 4.
- [14] Peng Y., Luxmoore I., Forster M. D., Cullis A. G., Inkson B. J.: 'Nanomanipulation and electrical behaviour of a single gold nanowire using in-situ SEM-FIB- nanomanipulators', *J. Phys. Conf. Ser.*, 2008, 126, article id 012031, p. 4.
- [15] Jun K., Jacobson J. M.: 'Programmable Growth of Branched Silicon Nanowires Using a Focused Ion Beam', *Nano Lett.*, 2010, 10, pp. 2777-2782.
- [16] Arkan E. F., Sacchetto D., Yildiz I., Leblebici Y., Alaca B. E.: 'Monolithic integration of Si nanowires with metallic electrodes: NEMS resonator and switch applications', *J. Micromech. Microeng.*, 2011, 21, article id 125018, p. 9.
- [17] Park B. C., Jung K. Y., Song W. Y., O B., Ahn S. J.: 'Bending of a Carbon Nanotube in Vacuum Using a Focused Ion Beam', *Adv. Mater.*, 2006, 18, pp. 95-98.
- [18] Romano L., Rudawski N. G., Holzworth M. R., Jones K. S., Choi S. G., Picraux S. T.: 'Nanoscale manipulation of Ge nanowires by ion irradiation', *J. Appl. Phys.*, 2009, 106, article id 114316, p. 6.
- [19] Borschel C., Spindler S., Lerose D., Bochmann A., Christiansen S. H., Nietzsche S., Oertel M., Ronning C.: 'Permanent bending and alignment of ZnO nanowires', *Nanotechnology*, 2011, 22, article id 185307, p. 9.
- [20] Jun K., Joo J., Jacobson J. M.: 'Focused ion beam-assisted bending of silicon nanowires for complex three dimensional structures', *J. Vac. Sci. Technol. B*, 2009, 27, 3043-3047.
- [21] Rajput N. S., Tong Z., Luo X.: 'Investigation of ion induced bending mechanism for nanostructures', *Mater. Res. Express*, 2015, 2, article id 015002, p. 8.
- [22] Tripathi S. K., Shukla N., Dhamodaran S., Kulkarni V. N.: 'Controlled manipulation of carbon nanopillars and cantilevers by focused ion beam', *Nanotechnology*, 2008, 19, article id 205302, p. 6.
- [23] Gour N., Verma S.: 'Bending of peptide nanotubes by focused electron and ion beams', *Soft Matter*, 2009, 5, pp. 1789-1791.
- [24] Yoshida T., Nagao M., Kanemaru S.: 'Characteristics of Ion-Induced Bending Phenomenon', *Jpn. J. Appl. Phys.*, 2010, 49, article id 056501, p. 5.
- [25] Rajput N. S., Banerjee A., Verma H. C.: 'Electron- and ion-beam-induced maneuvering of nanostructures: phenomenon and applications', *Nanotechnology*, 2011, 22, article id 485302, p. 7.
- [26] Yao N.: 'Focused Ion Beam Systems: Basics and Applications', (Cambridge University Press, New York, 2007), pp. 31.
- [27] Ziegler J. F., Ziegler M. D., Biersack J. P.: 'SRIM – The stopping and range of ions in matter (2010)', *Nucl. Instrum. and Meth. B*, 2010, 268, pp. 1818-1823.
- [28] Totten G. E., MacKenzie D. S.: 'Handbook of Aluminum: Physical Metallurgy and Processes', (CRC Press, New York, 2003), Vol. 1, pp. 220.